Ni-doped Hibonite (CaAl$_{12}$O$_{19}$): A New Turquoise Blue Ceramic Pigment

G. Costa[1], W. Hajjaji[2], M.P. Seabra[2], J. A. Labrincha[2], M. Dondi[3], G. Cruciani[4]

[1]*ESTG, Polytechnic Institute of Viana do Castelo, 4900-348 Viana do Castelo, Portugal*
[2]*Ceramics and Glass Engineering Department, CICECO, Univ. of Aveiro, 3810-193 Aveiro, Portugal*
[3]*Istituto di Scienza e Tecnologia dei Materiali Ceramici, CNR-ISTEC, 48018 Faenza, Italy*
[4]*Department of Earth Sciences, University of Ferrara, 44100 Ferrara, Italy*

Abstract. A new structure for ceramic pigments was synthesized by a conventional solid state reaction process. It is based on Ni-doped hibonite, CaAl$_{12}$O$_{19}$, which assumes a turquoise-like blue colour similar to that of V-doped zircon. Hibonite is associated with anorthite, CaAl$_2$Si$_2$O$_8$, acting like a fluxing agent in order to lower the synthesis temperature, and with cassiterite, SnO$_2$, acting as a tin buffer to promote coupled Ni^{2+} + Sn^{4+} → Al^{3+} + Al^{3+} substitution, in order to ensure the electric neutrality of the hibonite lattice. Since relatively low chromophore contents are required, this new system constitutes an interesting alternative to the common blue ceramic pigments based on cobalt aluminate spinel or vanadium-doped zircon, implying lower cost and environmental advantages. The pigments characterization was performed by X-ray powder diffraction, diffuse reflectance spectroscopy, CIELAB colourimetric analysis, and testing in ceramic glazes and bodies. The substitution of Al^{3+} by bigger ions, like Ni^{2+} and Sn^{4+}, increases the cell volume compared to undoped hibonite and is responsible of the turquoise blue colour, as verified by UV-Vis analysis. The chromatic mechanism is due to incorporation of Ni^{2+} in tetrahedral coordination, likely occurring at the site M3 of the hibonite lattice, where it partially substitutes the Al^{3+} ion. While this product shows a strong hue as a pigment, it is not stable after severe testing in glazes and attempts to improve its colouring performance are now under development.

Keywords: blue ceramic pigment, hibonite structure, nickel doping.

1. Introduction

The overall demand for blue ceramic pigments is growing with the production of ceramic products, especially glazes for wall and floor tiles as well as through-body coloration of unglazed porcelain stoneware. Available industrial blue pigments are vanadium-doped zircon V-ZrSiO$_4$, classified with the DCMA number 14-42-2, cobalt orthosilicate or olivine Co$_2$SiO$_4$, DCMA 5-08-2, and cobalt aluminate CoAl$_2$O$_4$, DCMA 13-26-2.[1-5] Cobalt aluminate is widely preferred to olivine, since a navy blue can be obtained with nearly half the actual CoO content (42 wt.% in CoAl$_2$O$_4$ against 71 wt.% in Co$_2$SiO$_4$), besides some differences in colour saturation.[2,3]

The most straightforward way to obtain blue colours in ceramics is by means of cobalt, which has been used since antiquity.[3] This solution has the advantage that Co^{2+} ions exhibit, when tetrahedrally coordinated, optical bands intensely absorbing the red-yellow light (500-700 nm) so resulting in highly saturated blue shades. The strong preference of Co^{2+} for CoO$_4$ tetrahedra, once dispersed in silicate and borosilicate glasses, implies no important colour changes if the pigment undergoes partial dissolution in glazes.[5]

However, the increasing price and limited availability of cobalt raw materials have made it important to minimize or even avoid the use of cobalt in the formulation of ceramic pigments.[5,6] In black spinels, the substitution of cobalt by nickel was successful,[7,8] involving also technological advantages, such as improved stability in Zn-rich glazes when

the substitution is partial,[2] and economic, since nickel is considerably more abundant than cobalt, and therefore less expensive.

Nevertheless, the development of a new, cobalt-free, blue pigment has to overcome the severe difficulty in finding a substitute, since Co^{2+} in non centrosymmetric sites (tetrahedral) assures the highest colouring efficiency known among crystal-field transitions.[9] Another transition ion capable of producing a blue coloration is Ni^{2+}, which gives turquoise shades once in non centrosymmetric ligand field.[6] The further step is searching for a stable structure which could accommodate Ni^{2+} in tetrahedral coordination. Because of the similar ionic radii of Ni^{2+} and Co^{2+} ions,[10] the substitution of cobalt by nickel should be the primary suggestion for current pigment structures, but $CoAl_2O_4$ is a normal spinel (i.e. cobalt in tetrahedral coordination) while nickel aluminate is an inverse spinel with most Ni in octahedral coordination.[11-12] On the other hand, the replacement of Co^{2+} by Ni^{2+} was successful in willemite, giving rise to turquoise shades.[6,13] Accordingly, a good starting point in the search for an alternative blue pigment would be to look for a stable structure with tetrahedral sites suitable to incorporate the Ni^{2+} ion. In order to respond to economic and environmental considerations, it is important to minimize the contents of this chromophore element, giving preference to the structures which originate solid solution pigments.

Calcium hexaluminate ($CaAl_{12}O_{19}$ or $CaO.6Al_2O_3$) occurs in nature as the mineral hibonite and presents the magnetoplumbite-type structure (space group P_{63}/mmc, Z=2) whose general crystallochemical formula is $A^{[12]} M1^{[6]} M2_2^{[5]} M3_2^{[4]} M4_2^{[6]} M5_6^{[6]} O_{19}$. Calcium occurs in 12-fold coordination (site A), whereas Al^{3+} ions are distributed over five different coordination sites, including three distinct octahedral (M1, M4 and M5), one tetrahedral (M3) and an unusual trigonal bipyramidal (M2) providing a five-fold coordination by oxygen ions.[14-17] Of great importance is the tendency of M^{2+} ions to be hosted at the M3 site, while M^{4+} and M^{5+} ions are preferentially accommodated at the M4 site.[16] In fact, the magnetoplumbite-group minerals may contain significant amounts of divalent as well as tetravalent and pentavalent cations.

The preference of divalent cations for the M3 site occurs because these substitutions are electrostatically more favourable than incorporation of highly charged cations.[16] This factor apparently predominates over the crystal field effects of the divalent transition metal ions: even Ni^{2+}, which possesses large octahedral crystal-field stabilization energy, shows a marked preference for a tetrahedral environment in this structure type.[18] The ions of different charges tend to improve the local charge balance in the crystal structure. Therefore, the introduction of divalent ions is thought to be achieved by coupled incorporation of tetravalent or pentavalent cations, which are mainly ordered over the octahedral sites in the face-sharing interlayer doublet.[16]

This ability to accommodate such a wide variety of ions, with different valence and coordination, makes the hibonite structure very interesting for potential use as a pigment. The electroneutrality of the hibonite lattice was eased by making available a tetravalent ion in order to get a coupled substitution: $Ni^{2+} \rightarrow Al^{3+}$ and $Sn^{4+} \rightarrow Al^{3+}$. Any excess of tin oxide is not detrimental for the overall pigment performance, since it ensures increased brightness. However, the temperatures required for its synthesis are too high for such applications. To overcome kinetic hindrances anorthite was introduced into the system, to lower the synthesis temperature of hibonite, allowing its application as pigment.

2. Experimental

Hibonite-based pigments, doped with NiO, were synthesized by the conventional ceramic route, producing a batch composition in the Al_2O_3-CaO-SiO_2-SnO_2 system (Table 1) corresponding approximately to 50% hibonite, 25% anorthite and 25% cassiterite (quoted

as T1-St). The following precursors were used in batch formulations: Calcite (Calcitec M1), Silica sand (Sibelco P500), Wollastonite (49.6% CaO, 48.9% SiO_2 and 0.7% MgO), Alumina (Alcoa, CT 3000), Tin oxide (CCT, MP 989), and Nickel oxide (Aquitex, 99.9% NiO and 0.1% SiO_2).

Furthermore, a galvanizing sludge, coming from the Cr/Ni plating process (C-sludge) was collected and used, after disintegration and drying at 100°C, as low cost nickel source (pigment T1-Cs). The waste was characterized by determining chemical composition (XRF, Philips X'UNIQUE II) and phase composition (XRD, Rigaku Geigerflex D/max – Series). C-sludge is produced by the physico-chemical treatment of wastewaters generated by a Ni/Cr plating plant. Its chemical composition is on average (wt.%.): 0.23 Al_2O_3, 0.53 Fe_2O_3, 33.17 NiO, 14.49 Cr_2O_3, 3.15 SiO_2, 0.60 CaO, 1.41 Na_2O, 2.13 ZnO, 0.86 SO_4, 6.33 other components (Co not detected) and 37.10 loss of ignition at 1000ºC.

In order to obtain fine and homogeneous slurries, the mixtures were wet ball-milled in ethanol for 1 hour, then dried at 110°C and calcined in an electric kiln at 1300, 1400, and 1450 or 1500°C (3 hours dwell time and 5°C/min. heating rate). Calcined powders were manually disintegrated and characterized by X-ray diffraction (XRD) by using a Bruker D8 Advance diffractometer, equipped with a Si(Li) solid state detector (Sol-X), using CuKα radiation. Rietveld refinements of XRD patterns were performed using the GSAS and EXPGUI softwares. Thirty-two independent variables were refined: scale-factors, zero-point, 15 coefficients of the shifted Chebyschev function to fit the background, unit cell dimensions, profile coefficients (1 Gaussian, GW, and 2 Lorentzian terms, LX and LY). The number of variables and the figures of merit of Rietveld refinements are reported in Table 2.

The microstructure and chemical homogeneity of the pigments were studied by scanning electron microscopy (SEM, Hitachi, S4100) with energy-dispersive X-ray spectroscopy (EDS).

Measurements of the CIELAB colour parameters were also conducted using a Konica Minolta Chroma Meter CR-400. This method uses the reflectance data in the visible region to obtain the three relevant parameters, L*a*b*, measuring respectively the brightness, red/green and yellow/blue hue intensities. Diffuse reflectance spectroscopy (DRS) was performed with a Perkin Elmer λ35 spectrophotometer in the 300-1100 nm range (0.03 nm step) using a $BaSO_4$ integrating sphere and white reference material. Reflectance (R_∞) was converted to absorbance (K/S) by the Kubelka-Munk equation: $K/S=(1-R_\infty)^2/2R_\infty$, and the optical spectra were deconvoluted using gaussian bands (PFM, OriginLab).

Finally, to evaluate the colour development in common ceramic products, each pigment was added to:

(a) at 5 wt.% to commercial glazes and fired at 1050ºC; *(i)* a transparent and bright lead-free glaze referred as **TB** (SiO_2, Al_2O_3, B_2O_3, CaO as main constituents >8 %, 2-8% Na_2O, and <2% K_2O); *(ii)* an opaque and bright glaze, referred as **OB** (SiO_2, B_2O_3, ZrO_2 as main constituents >8 %, 2-8% Al_2O_3, Na_2O, CaO, and <2% K_2O, MgO, ZnO, CoO); *(iii)* a transparent and matt glaze, referred as **TM** (SiO_2, ZnO, PbO as main constituents >8 %, 2-8% Al_2O_3, B_2O_3, CaO, Na_2O, and <2% K_2O, MgO); *(iv)* an opaque matt glaze, referred as **OM** (SiO_2, Al_2O_3, CaO, ZrO_2, ZnO as main constituents >8 %, 2-8% Na_2O, B_2O_3, PbO and <2% K_2O, MgO).

(b) at 10 wt.% to porcelain stoneware ceramic bodies, to be fired at 1200ºC, referred as **CB**.

The mixtures were prepared by a wet ball-milling method for 30 min. and were dried at 110°C. The powders were then used to press pellets (Ø = 2.5 cm) that were put in alumina crucibles and fired (30 min dwell time and 5°C/min heating rate) in an electric furnace in air.

3. Results and discussion

3.1. Phase composition

An increased pigment yield was observed for increasing synthesis temperatures: XRD patterns show – along with the main constituents hibonite $CaAl_{12}O_{19}$, anorthite $CaAl_2Si_2O_8$, and cassiterite SnO_2 – secondary phases, like corundum Al_2O_3 and gehlenite $Ca_2Al_2SiO_7$, which are present at the lower calcination temperatures, but have disappeared or are minimized at the highest one (Fig. 1).

The optimum temperature of calcination was set to 1450ºC for T1-Cs because of its sintering, while T1-St was still easily disagglomerated after calcining at 1500°C. The best pigments consist of hibonite (55-57%), anorthite (~24%) and cassiterite (16-17%) with minor gehlenite (~3%), as given in Table 2. Therefore, there is a considerable deviation from the phase composition predicted by batch formulation: ~50% hibonite, ~25% cassiterite and ~25% anorthite. Since the peaks of hibonite are significantly displaced in the pigments, when compared with the pure phase, part of the tin oxide is likely accommodated into the hibonite lattice. No free nickel oxide was detected; this seems to indicate that Ni is mostly inside the hibonite structure. Both these aspects will be discussed in some detail in the paragraph 3.2.

3.2. Hibonite crystal structure

The unit cell parameters of hibonite are compared with synthetic $CaAl_{12}O_{19}$ to avoid multiple effects of variable elements (Ce, Ti, Mg, Fe, Si, La, etc.) present in natural hibonite (Table 3).[15,17] The a/c ratio of Ni-doped hibonite decreases from synthetic hibonite to sample T1-Cs and T1-St along with an increase in unit cell volume; this implies that the hibonite unit cell becomes more elongated in the [001] direction, likely because Al^{3+} is substituted by bigger ions like Ni^{2+} and Sn^{4+}. The mean metal-oxygen distances are listed in Table 3, comparing Ni- and Sn-doped pigments with undoped hibonite. Doping exerts a strong influence on the mean M-O distance in the M4 and M1 octahedral sites, while little effect can be seen in the other sites. In fact, the mean M-O distance in M4 increases from 1.92 Å in undoped hibonite to 1.97 Å in T1-Cs and even to 2.02 Å in T1-St; such growth is consistent with a partial substitution of Al^{3+} (ionic radius 0.535 Å in sixfold coordination) with Sn^{4+} and/or Ni^{2+} (both i.r. 0.69 Å).[10] The mean metal-oxygen distance remains unchanged in the M5 site, which is known to accommodate almost exclusively aluminium in natural hibonites.[16] Both the tetrahedral site M3 and the trigonal bipyramidal M2 site exhibit mean M-O distances that are shorter than those observed in undoped hibonite.

3.3. SEM/EDS analysis

Figure 2 shows the microstructure and element distribution on particles of the sample T1-St. The small grain sizes and their morphology (the dimensions of the plate-like particles are on average 2.25 μm × 0.75 μm) make it difficult to discriminate between hibonite and anorthite on the basis of EDS chemical analysis, due to the analogy of composition (minor silicon may also be present in hibonite). The SEM characterization reveals three distinct phases in this sample, marked by points A, B and C, whose EDS analyses are presented in Table 4.

The grain of intermediate gray tone (A) exhibits the highest alumina-to-calcium ratio and a low content of silicon. In the element mapping, it can be clearly seen a zone with a higher alumina concentration combined with low amounts of silicon and calcium, indicating it is composed of hibonite. Nickel occurs in the areas attributed to hibonite (the only phase which reveals some nickel by EDS). In these grains, a minor amount of tin was also detected. The Al/Ca ratio appears to be lower than expected for pure hibonite, even by accounting all elements that might replace Al in the structure (Ni, Sn, and Si), implying a

deviation from the stoichiometric composition (or analytical interference from Ca-rich surrounding phases, such as anorthite).

The darker phase in Figure 2 (B) appears to be widely distributed and apparently surrounding the other grains. It shows the greatest levels of silicon and calcium with respect to alumina, indicating we are likely dealing with anorthite-rich zones (since the stoichiometry is not strictly respected).

The light-coloured phase (C) is identified as cassiterite due to its high content of tin and acicular morphology.[6] In both cassiterite and anorthite phases, no traces of nickel were detected by coupled SEM/EDS analysis.

3.4. Optical spectroscopy

The visible diffuse reflectance spectra of the samples T1-St and T1-Cs present some similarities and are shown in Figure 3. Both pigments are characterized by a relatively intense absorption in the 550-650 nm range, with maximum reflectance observed at 450 nm (blue hue) and 490 nm (green-blue hue), but T1-St shows a higher saturation and a better colour purity (Table 5). This suggests that the occurrence of further transition metal cations (i.e. Cr^{3+} from the sludge in the T1-Cs pigment) may determine the chromatic differences registered in these two samples. The resulting colour is a characteristic turquoise analogous to those obtained by Ni-doping of willemite or V-doping of zircon.[4,6]

The optical spectra consist of several bands ascribable to the presence of Ni^{2+} in tetrahedral coordination (Figure 4). The intense bands in the visible spectrum at 16.000-18.000 cm^{-1} are responsible for the turquoise blue colour and can be assigned to the v_3 spin-allowed transition: from the ground state $^3T_1$ (^3F) to $^3T_1$ (^3P), expressed according to the regular tetrahedron T_d point symmetry (Table 6). Since the tetrahedral M3 site of hibonite has a lower point symmetry (C_{3v}) it implies that this transition undergoes a splitting in two terms: $^3A_2$ and ^3E; further splitting (bands 4-5-6 in Fig. 4) arises from spin-orbit coupling frequently occurring in d^8 ions like Ni^{2+}.[19-21] Weaker bands are attributed to spin-forbidden transitions from ^1G and ^1D terms on the high and the low energy sides, respectively; broad bands (e.g. numbers 3, 7 and 8 in Fig. 4) are probably due to splitting of transitions $^1T_2$ (^1D and ^1G) and $^1T_1$ (^1G). The near infrared band centred near 8.000 cm^{-1} is assigned to the v_2 transition $^3T_1$ (^3F) → $^3A_2$ (^3F).[19-21] This interpretation is in reasonable agreement with energy values calculated according to the crystal field theory by means of the following optical parameters: crystal field strength 450 cm^{-1}, Racah B 920 cm^{-1} and C 3800 cm^{-1} (Table 6).

There is an apparent discrepancy between the spectroscopic evidence of Ni^{2+} in fourfold coordination and the X-ray diffraction data showing a short metal-oxygen mean distance for the tetrahedral site M3 of hibonite lattice, not consistent with a Ni-Al substitution. However, optical spectroscopy is highly sensitive, particularly when electron transitions occur in a non centrosymmetric site, and is able to detect an amount of Ni^{2+} in tetrahedral coordination that is below the detection limit for XRD.

3.5. Technological testing

The best turquoise colour was achieved in both T1-St and T1-Cs samples at the maximum firing temperature (Table 5), as shown by the highest negative values for the chromatic parameters b* (blue) and a* (green), as well as the lowest L* (brightness). The T1-St pigment exhibits the best colour, with an extremely high blue component (b* = -48) and a relatively low green component (a* = -4) with respect to the sludge-based T1-Cs pigment, which is less blue (b* = -18) and greener (a* = -10). The colour coordinates of T1-St and T1-Cs pigments are in the range of commercialized vanadium zircon formulations.[4]

Table 5 also shows the colourimetric parameters of sintered pigments after application in glazes and ceramic bodies (Figure 5). The blue component is to a large extent lost, while

the green component is substantially maintained. This behaviour is consistent with diffusion of Ni^{2+} ions in the vitreous matrix as consequence of hibonite breakdown (in the fired glaze there is only cassiterite as crystalline phase, Fig. 6). This probably happens because of the severe conditions (long firing time and slow thermal rate). An attempt to improve hibonite stability is now under study by using Ti co-doping. The use of this versatile structure in the formulation of solid solution pigments will be investigated to determine the performance with other chromophore elements, such as cobalt.

4. Conclusions

A new turquoise blue ceramic pigment has been developed on the basis of nickel-doped hibonite. Although the ability of $CaAl_{12}O_{19}$ to incorporate a variety of ions in different coordinations and valences is already recognized, the application of hibonite as a pigment is novel, the main hindrance being the high temperatures required for its synthesis. However, when anorthite is included in the system, the temperature of hibonite crystallization is significantly reduced. The presence of cassiterite acts as a source of tetravalent tin, which is necessary to ensure the electrical neutrality of doped-hibonite by compensated the charge mismatch of Ni^{2+}-Al^{3+} substitution with Sn^{4+}-Al^{3+}. The increase of hibonite unit cell volume is consistent with the substitution of small Al^{3+} ions with larger Ni^{2+} and Sn^{4+} ions. Evidence for Sn incorporation in the octahedral M4 and M1 sites comes from the metal-oxygen distances. However, the turquoise blue colour, similar to that of V-doped zircon and Ni-doped willemite pigments, is consistent with the occurrence of Ni^{2+} ions in tetrahedral coordination in the hibonite lattice. Such a mechanism involves the incorporation of a low amount of nickel in partial substitution of Al^{3+} in the M3 site, which is conspicuous from optical spectroscopy but not detectable by X-ray diffraction. Hibonite pigments seem to be unstable after sever testing in glazes and attempts to improve its colouring performance are now under way.

Acknowledgement

References

[1] Italian Ceramic Society, Colour, Pigments and Colouring in Ceramics, SALA, Modena 2003.

[2] Escribano P., Castelló J.B.C., Cordoncillo E.C., Esmaltes y pigmentos cerámicos. Castellón, Faenza Editrice Ibérica S.L., 2001.

[3] Eppler R. & Eppler D., Glazes and Glass Coating, The American Ceramic Society, Westerville, Ohio, 2000.

[4] Caselli C., Lusvardi G., Malavasi G., Menabue L., Miselli P., Multitechnique approach to V–ZrSiO4 pigment characterization and synthesis optimization. J. Eur. Ceram. Soc., 2007, 27 1743-1750.

[5] Llusar M., Forés A., Badenes J.A., Calbo J., Tena M.A., Monrós G., Colour analysis of some cobalt-based blue pigments. J. Eur. Ceram. Soc., 2001, 21, 1121-1130.

[6] Forés A., Llusar M., Badenes J.A., Calbo J., Tena M., Monrós G., Alternative turquoise blue pigment for glazes. Am. Ceram. Soc. Bull., 2001, 80, 47-52.

[7] Eppler R.A., Cobalt-free black pigment. Ceram. Bull., 1981, 60, 562-565.

[8] Eppler R.A., Nickel spinels. Ceram. Bull., 1982, 61, 847-850.

[9] Forés A., Llusar M., Badenes J.A., Calbo J., Tena M., Monrós G., Cobalt minimization in willemite ($Co_xZn_{2-x}SiO_4$) ceramic pigments. Green Chemistry, 2000, 2, 93-100.

[10] Shannon R.D., Revised effective ionic radii and systematic studies of interatomic distances in halides and chalcogenides. Acta Cryst., 1976, A32, 751-767.

[11] Monrós G., Badenes J.A., García A., Tena M.A., El color de la cerámica: Nuevos mecanismos en pigmentos para los nuevos procesados de la industria cerâmica, Publicacions de la Universitat Jaume I, Castelló de la Plana, 2003.

[12] Shriver D.F. & Atkins P.W., Inorganic Chemistry, Oxford University Press, 3th ed., Oxford, 1999.

[13] Brunold T., Güdel H.U., Cavalli E., Optical spectroscopy of Ni^{2+} doped crystals of Zn_2SiO_4. Chem. Phys. Lett., 1997, 268, 413-420.

[14] Domínguez C., Chevalier J., Torrecillas R., Fantozzi G., Microstructure development in calcium hexaluminate. J. Eur. Ceram. Soc., 2001, 21, 381-387.

[15] Burns R.G. & Burns V.M., Crystal chemistry of meteoritic hibonites. J. Geophys. Res., 1984, 89, B14, C313-C322.

[16] Bermanec V., Holtstam D., Sturman D., Criddle A.J., Back M.E., Šćaviničar S., Nežilovite. A new member of the magnetoplumbite group, and the crystal chemistry of magnetoplumbite group, and the crystal chemistry of magnetoplumbite and hibonite. Can. Mineral., 1996, 34, 1287-1297.

[17] Hofmeister A.M., Wopenka B., Locock A.J., Spectroscopy and structure of hibonite, grossite, and $CaAl_2O_4$: implications for astronomical environments. Geochim. Cosmochim. Ac., 2004, 68, 4485-4503.

[18] Laville F., Perrin M., Lejus A.M., Gasperin M., Moucorge R., Vivien D., Synthesis, crystal growth, structural determination and optical absorption spectroscopy of the magnetoplumbite type compound $LiNiAl_{11}O_{19}$. J. Solid State Chem., 1986, 65, 301-308.

[19] Lever A.B.P., Inorganic Electronic Spectroscopy, Elsevier, 2nd ed., Amsterdam, 1984.

[20] Utsunomiya A., Tanaka K., Morikawa H., Marumo F., Kojima H., Structure refinement of CaO 6(Al_2O_3). J. Solid State Chem., 1988, 75, 197-200.

[21] Solntsev V.P., Tsvetkov E.G., Alimpiev A.I., Mashkovtsev R.I., Coordination and valence state of nickel ions in beryl and chrysoberyl crystals. Phys. Chem. Miner., 2006, 33, 300-313.

Table 1 − Prepared pigment formulations.

Reference	Composition	Al_2O_3	$CaCO_3$	SiO_2	SnO_2	NiO	C sludge
	Molar ratio	2.62	1	1	1	0.12	-
T1-St	wt.(%)	45.9	16.9	10.2	25.5	1.5	-
T1-Cs	wt.(%)	44.9	16.8	10.1	25.3	-	2.9

Table 2 – Phase composition and figures of merit of Rietveld refinements of T1-St and T1-Cs pigments.

Phase composition (wt. %)	T1-St	T1-Cs
Hibonite 5H	56.8(2)	54.9(2)
Anorthite	23.7(2)	24.5(2)
Cassiterite	16.1(2)	17.0(2)
Gehlenite	3.4(2)	3.6(2)
Number of data	3750	3751
Number of variables	61	64
Number of observations	3744	3768
R_{wp} (%)	7.9	9.3
R_p (%)	5.8	6.6
R(B) hibonite only (%)	3.6	2.7

Table 3 – Hibonite unit cell parameters and mean metal-oxygen distances. Comparison of T1-St and T1-Cs pigments with literature data.

Phase composition	Unit	T1-St	T1-Cs	Hibonite[17]	Hibonite[15]
Unit cell parameter a	Å	5.585(1)	5.579(1)	5.566(1)	5.564(2)
Unit cell parameter c	Å	22.093(1)	22.047(1)	21.923(4)	21.892(5)
Unit cell volume V	Å^3	596.8(1)	594.3(1)	588.1(1)	586.9(1)
Site A (coord. 12)	Å	2.676(1)	2.744(1)	2.749	2.748
Site M1 (coord. 6)	Å	1.925(6)	1.901(8)	1.880	1.879
Site M2 (coord. 4+)	Å	1.793(2)	1.794(2)	1.826	1.824
Site M3 (coord. 4)	Å	1.771(8)	1.799(7)	1.802	1.799
Site M4 (coord. 6)	Å	2.022(5)	1.965(9)	1.919	1.915
Site M5 (coord. 6)	Å	1.907(5)	1.907(7)	1.909	1.907

Table 4 – EDS analysis of some grains showed in the SEM micrograph (see Figure 3) of the T1-St /1450°C. Molar ratios of relevant elements were also determined.

Elements (mol. %)	A	B	C	Cassiterite	Anorthite	Hibonite
O	63.3	64.9	82.75	66.7	61.6	59.4
Al	29.4	18.2	0.74		15.4	37.5
Ca	2.99	2.93	0.79		7.69	3.12
Si	0.99	11.4	0.13		15.4	
Sn	1.83	2.61	15.6	33.3		
Ni	1.50	-	-			
Molar ratios						
Al/Ca	9.83	6.21	-		2	12
Al/ Si	0.034	0.625	-		1.00	
(Al+Sn+Si+Ni)/Ca	11.28					

Table 5 – L*a*b* values for the sintered pigments and their applications.

Reference		T1-Cs			T1-St		
	Temp.(ºC)	L*	a*	b*	L*	a*	b*
Pigment	1300	67.6	-6.0	-11.3	71.6	-8.2	-15.4
	1400	66.5	-8.3	-16.2	64.9	-7.2	-33.4
	1450	66.2	-10.3	-18.1	-	-	-
	1500	-	-	-	60.7	-4.4	-48.0
Transparent bright glaze (TB)	1050	66.0	-8.6	+5.3	62.8	-9.5	-0.4
Opaque bright glaze (OB)	1050	86.1	-4.4	+0.6	84.8	-5.8	-3.1
Transparent matt glaze (TM)	1050	69.0	-6.2	+8.9	66.0	-8.5	+2.2
Opaque matt glaze (OM)	1050	83.4	-4.7	-1.6	82.4	-7.2	-6.7
Porcelain stoneware body (CB)	1200	72.9	-3.6	+3.7	71.4	-6.1	-0.9

Table 6 – Deconvolution of the DRS spectrum of the sample T1-St (see figure 4). Bands are attributed to electron transitions of Ni^{2+} in tetrahedral coordination.

Band No.	Transition from ground state $^3T_1\,(^3F)\rightarrow$		Peak centroid (cm^{-1})	
	T_d	C_{3v}	experimental	calculated*
1	$^3A_2\,(^3F)$	^3A	8280	8290
2	$^1T_2\,(^1D)$	$^1A_1 + {}^1E$	12870	12920
3	$^1E\,(^1D)$	^1E	14220	14050
4		$^3A_2$	15920	
5	$^3T_1\,(^3P)$		16840	16890
6		^3E	17890	
7	$^1T_2\,(^1G)$	$^1A_1 + {}^1E$	20300	-
8	$^1T_1\,(^1G)$	$^1A_2 + {}^1E$	24320	22430
9	$^1A_1\,(^1G)$	$^1A_1$	26650	-
10	Ni-O charge transfer		30400	-

*Band energy calculated for Dq=450 cm^{-1}, Racah B=920 cm^{-1} and C=3800 cm^{-1}.
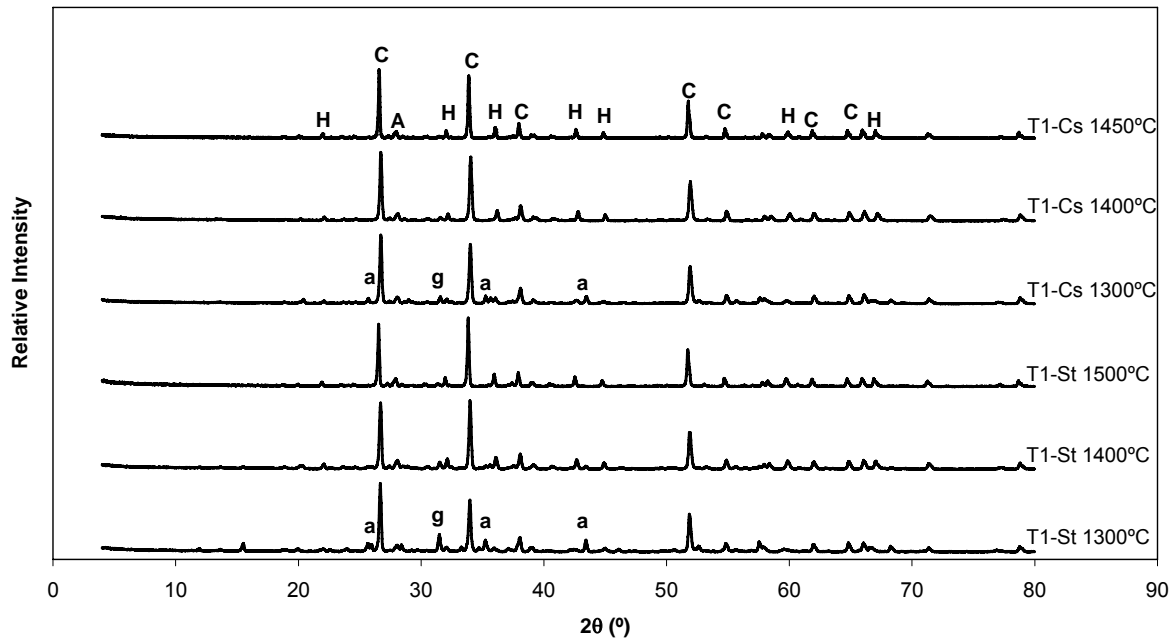
Figure 1 – XRD patterns of T1-Cs (calcined at 1300, 1400 and 1450ºC) and T1-St (calcined at 1300, 1400 and 1500ºC). The identified phases are: A- anorthite; C- cassiterite; H- hibonite; a-alumina and g- gehlenite.
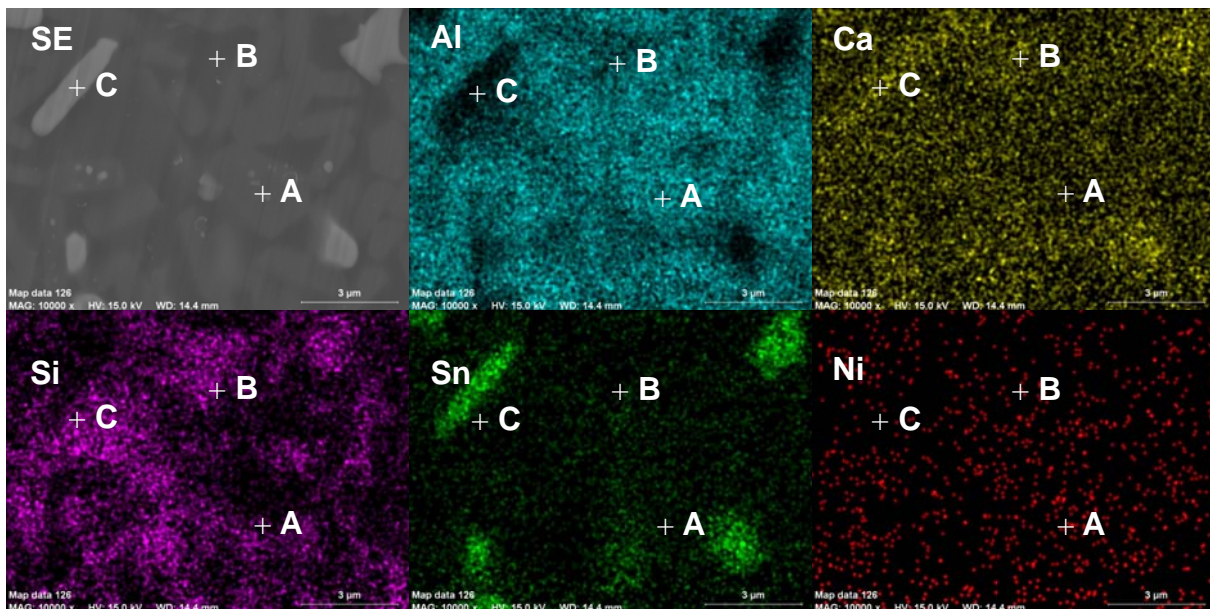

Figure 2 – SEM-EDS analysis of T1-St sintered at 1450°C; green = cassiterite; pink = anorthite; darker zones = hibonite grain).
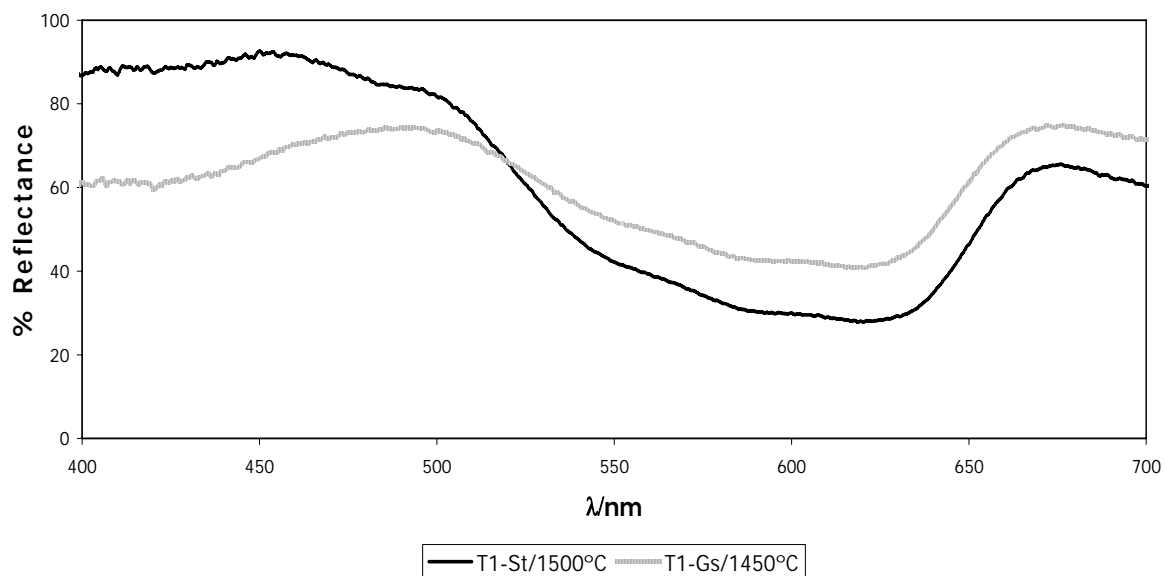
Figure 3 –UV-Vis reflectance spectra of T1-St and T1-Cs pigments, fired respectively at 1500 e 1450ºC.
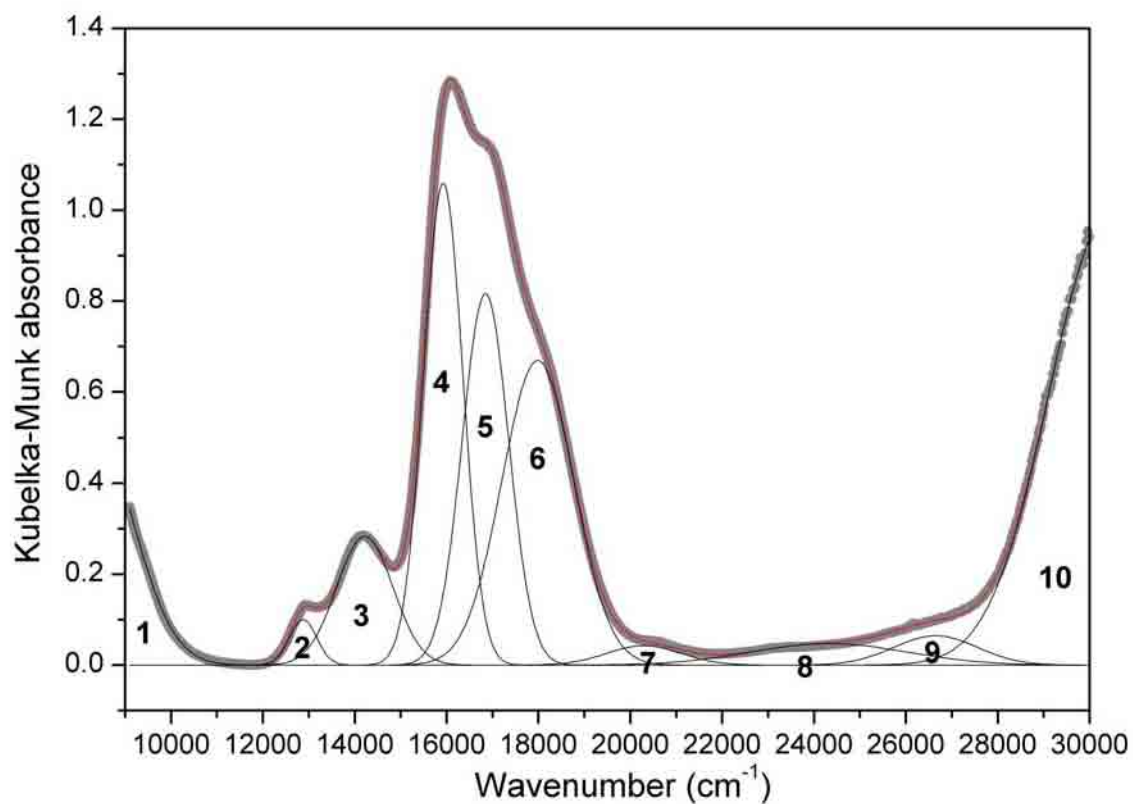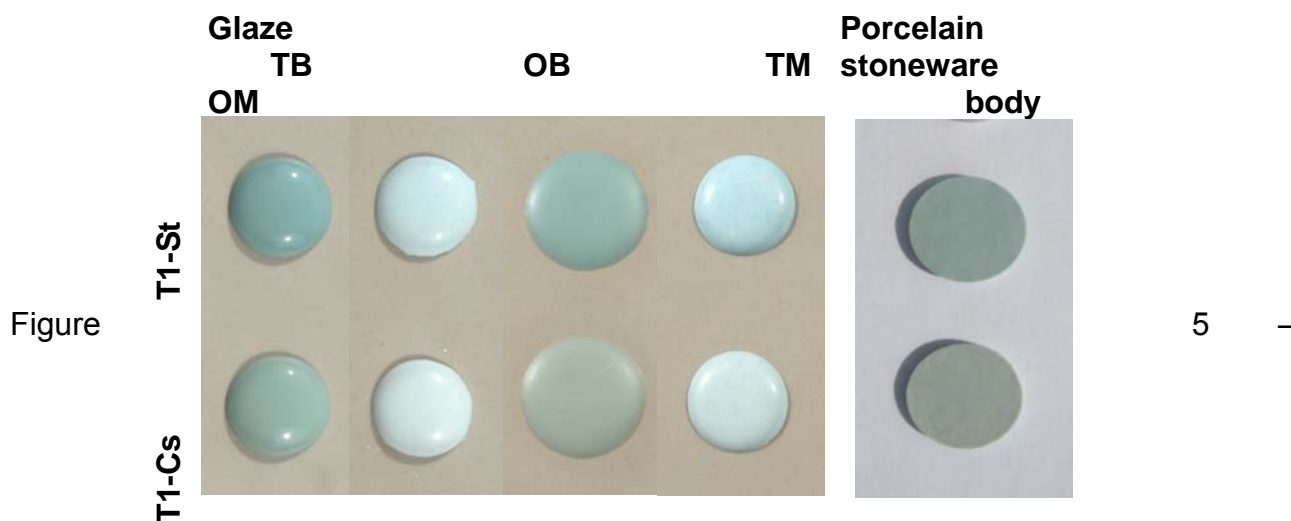

Figure 4 – Deconvoluted DRS spectrum of the T1-St pigment calcined at 1500ºC. Bands are numbered with reference to Table 5.

Figure 5 –

Colours developed by glazes containing 5 wt.% pigments (transparent bright glaze TB, opaque bright glaze OB, transparent matt glaze TM, opaque matt glaze OM) and by the porcelain stoneware body containing 10 wt.% pigments (T1-St-1500ºC or T1-Cs-1450ºC).
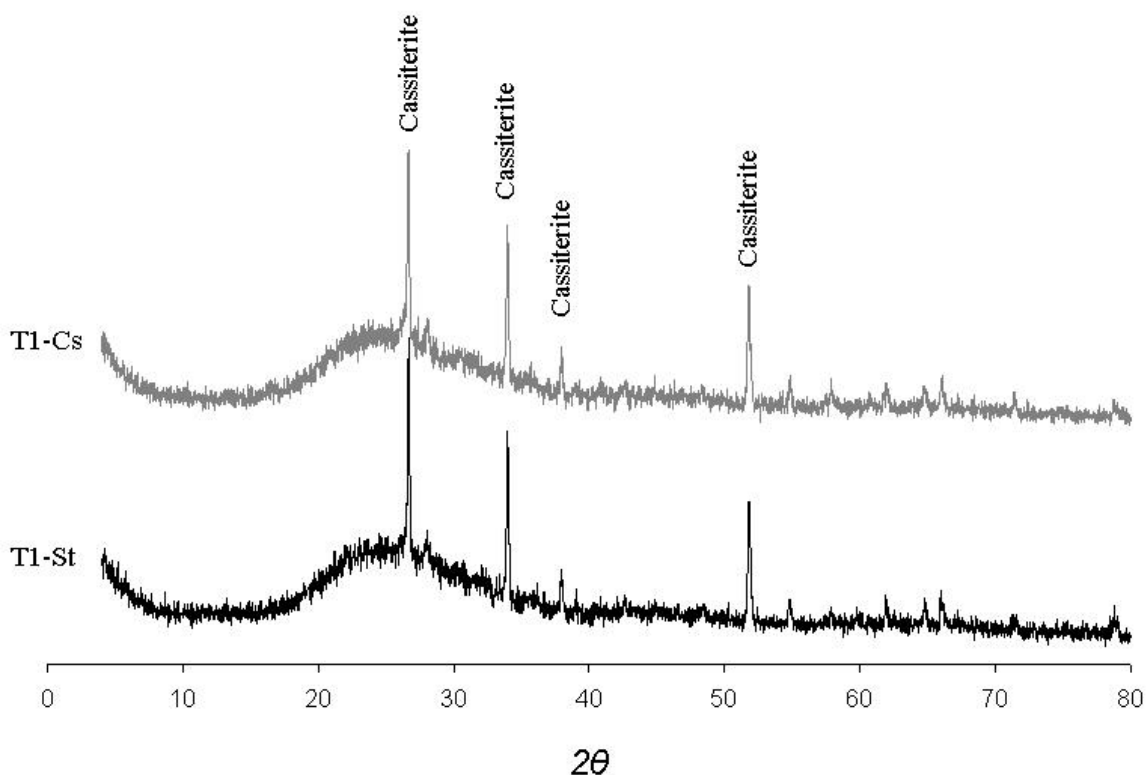

Figure 6 – XRD patterns of T1-St and T1-Cs pigments applied in transparent glazes.